Experimental study on the effects of two-dimensional surface defects on the transition of a sucked boundary-layer

Jeanne Methel, Maxime Forte, Olivier Vermeersch, Grégoire Casalis

▶ **To cite this version:**

Jeanne Methel, Maxime Forte, Olivier Vermeersch, Grégoire Casalis. Experimental study on the effects of two-dimensional surface defects on the transition of a sucked boundary-layer. Aero 2020+1 - 55th 3AF International Conference on Applied Aerodynamics, Association 3AF - Association Aéronautique et Astronautique de France, Apr 2021, Online, France. pp.FP82-AERO2020-Forte. hal-03206545

HAL Id: hal-03206545
https://hal.science/hal-03206545

Submitted on 23 Apr 2021

HAL is a multi-disciplinary open access archive for the deposit and dissemination of scientific research documents, whether they are published or not. The documents may come from teaching and research institutions in France or abroad, or from public or private research centers.

L'archive ouverte pluridisciplinaire **HAL**, est destinée au dépôt et à la diffusion de documents scientifiques de niveau recherche, publiés ou non, émanant des établissements d'enseignement et de recherche français ou étrangers, des laboratoires publics ou privés.

55th 3AF International Conference on Applied Aerodynamics
23 – 25 March 2020, Poitiers - France

FP82-AERO2020-Forte

EXPERIMENTAL STUDY ON THE EFFECTS OF TWO-DIMENSIONAL SURFACE DEFECTSON THE TRANSITION OF A SUCKED BOUNDARY-LAYER

Jeanne Methel [(1)], Maxime Forte[(2)], Olivier Vermeersch[(3)] and Grégoire Casalis[(4)]
[(1)] *ONERA/DMPE, Université de Toulouse, F-31055 Toulouse, France*
[(2)] *ONERA/DMPE, Université de Toulouse, F-31055 Toulouse, France, Email: maxime.forte@onera.fr*
[(3)] *ONERA/DMPE, Université de Toulouse, F-31055 Toulouse, France, Email: olivier.vermeersch@onera.fr*
[(4)] *ISAE-Supaero, Université de Toulouse, F-31055 Toulouse, France, Email: gregoire.casalis@isae-supaero.fr*

ABSTRACT

As laminar flow control by boundary layer suction is becoming an increasingly viable commercial application, airframe integration issues still need to be addressed. The current implementation of wall suction on an aerodynamic surface involves the juxtaposition of a perforated suction panel next to a solid-wall panel: at the junction, destabilizing surface imperfections are expected to occur. The competition between wall suction and surface defects therefore needs to be investigated to understand if current manufacturing tolerances are acceptable to justify the implementation of wall suction. The focus of this experimental study is to investigate the effect of surface defects on the laminar-turbulent transition of a sucked boundary layer. The objective is to provide critical height criteria below which suction could be effective. A flat plate with a suction region was placed in a two-dimensional Blasius flow, and surface defects were introduced in the form of wires and forward-facing steps (FFS). For both types of defect, the (critical) dimensions for which transition occurred at the defect location were unchanged, regardless of the use of wall suction. However, suction remained effective in delaying transition in the presence of subcritical defects, a favorable argument for this technology's implementation as tolerances on aerodynamic surfaces improve.

1. INTRODUCTION

While air traffic volume is projected to increase, the aviation industry is also faced with the need to reduce its fuel consumption for environmental sustainability, leading to a renewed interest in laminar flow control (LFC) research. One LFC technology consists in stabilizing the boundary layer using wall suction, most commonly through a micro-perforated suction panel or porous wall. Applying wall suction on a boundary layer increases its mean velocity profile curvature (and therefore its stability), and redistributes the disturbance energy closer to the wall where there is higher viscous dissipation. As a result, the growth of boundary layer instabilities is reduced and transition is delayed.
This technology has proven effectiveness as shown through numerous experimental investigations [1-2] and numerical studies [3-5]; however, attempts to develop a simple approach, such as the e^N method, on results from HLFC flight tests [6] were unsatisfactory in providing accurate transition prediction. Based on these studies, wall suction modeling still requires sophisticated numerical tools [7] that cannot easily be incorporated in the aircraft design cycle.

In addition to this issue, current manufacturing techniques do not allow to conceive the implementation of a wall suction technology without introducing surface defects (e.g., gaps, forward- and backward-facing steps) at the junction between the porous and solid wall regions. Surface defects generally tend to destabilize the boundary layer either by modifying local receptivity, further amplifying existing instabilities or changing the mean flow stability by introducing inflection points in the mean velocity profile because of the small separation bubbles that can form around a defect. Transition criteria were also determined for surface defects such as gaps, forward- and backward-facing steps on "natural" boundary layers, i.e., without suction [8-9]. However, experimental data are currently not available in the open literature to determine whether or not a boundary layer

with suction behaves similarly to one without suction in the presence of a surface defect. Additional investigations are therefore required to further understand the combined effects of wall suction and surface defects on boundary layer stability. With this additional information, transition prediction models can then be modified to account for this interaction more accurately.

The objective of the present study is therefore to perform an experimental characterization of the combined effects of surface defects (wires and forward-facing steps) and wall suction on the laminar-turbulent transition of a boundary layer in two-dimensional incompressible flow. First the experimental facility in which the present investigation was performed is presented, followed by a brief description of the stabilizing effects of wall suction in the smooth (no defect) case. Finally, the combined effects of surface defects and wall suction are characterized both experimentally and numerically.

2. EXPERIMENTAL FACILITY

This study was conducted in the ONERA TRIN 2 subsonic wind tunnel, shown in Fig. 1, operating at local atmospheric conditions. Test section speeds range from 20 $m.s^{-1}$ to 50 $m.s^{-1}$, corresponding to equivalent unit Reynolds numbers between $1x10^6$ m^{-1} and $3x10^6$ m^{-1}. In the present study, all measurements were performed at the single nominal unit Reynolds number of $2.6x10^6$ m^{-1}. This facility is suited to laminar-turbulent transition experiments because the test section is decoupled from the driving fan located at the wind tunnel exhaust by a noise-reduction chamber (not shown in Fig. 1). The purpose of this chamber is to prevent pressure waves from the fan from propagating upstream into the test section. All the walls, floor and ceiling of the noise-reduction chamber are lined with foam and a partition obstructs the flow path between the diverging nozzle exit and the wind tunnel exhaust to create an additional obstacle to the upstream-travelling pressure waves from the fan. The resulting freestream turbulence levels, although dependent on test section speed, are consequently always below 0.18% (evaluated over frequencies ranging from 3 Hz to 10 kHz).

A flat plate model with a numerically-optimized leading edge was mounted, spanning the entire width of the test section (0.4 m) and with total length of 1.10 m. The suction region starts 0.18 m from the leading edge and is divided in nine suction chambers, each 0.048 m (x) long by 0.019 m (y) deep and separated by 0.002 m (x) stringers, totaling in a streamwise length of approximately 0.450 m. Additionally, the suction region is 0.350 m (z) in the spanwise direction. Chamber C1 is closest to the leading edge, while chamber C9 is furthest downstream. A general layout of the flat plate with the suction region and the coordinate system is given in Fig.2. Further details about the facility and model can be found in [10].

The flat plate and flap angles of attack were set to have as close as possible to a zero pressure gradient over the entire plate's length (excluding the leading edge region) to obtain Blasius flow on the upper side. The presence of two-dimensional flow was also verified. The relatively low free-stream turbulence of the wind tunnel coupled to the flat plate with zero pressure gradient indicated that the traditional path to transition mainly driven by the linear amplification of primary modes, as defined by [11], would occur. Experimental verification confirmed that transition was indeed the result of the linear amplification of Tollmien-Schlichting (TS) waves, as shown on Fig. 3. In this figure, the profiles are acquired over the flat plate with a solid panel over the suction region at a streamwise position 558 mm from the leading edge. At this position, located upstream of the transition position (at x equal to 740 mm, corresponding to a transition Reynolds number of $1.92x10^6$, the TS instabilities are amplified enough to be identified, as shown in Fig. 3b. The experimental profile (evaluated by integrating the velocity fluctuations spectrum over chosen frequencies) shows relatively good agreement with the eigenfunction of the streamwise velocity

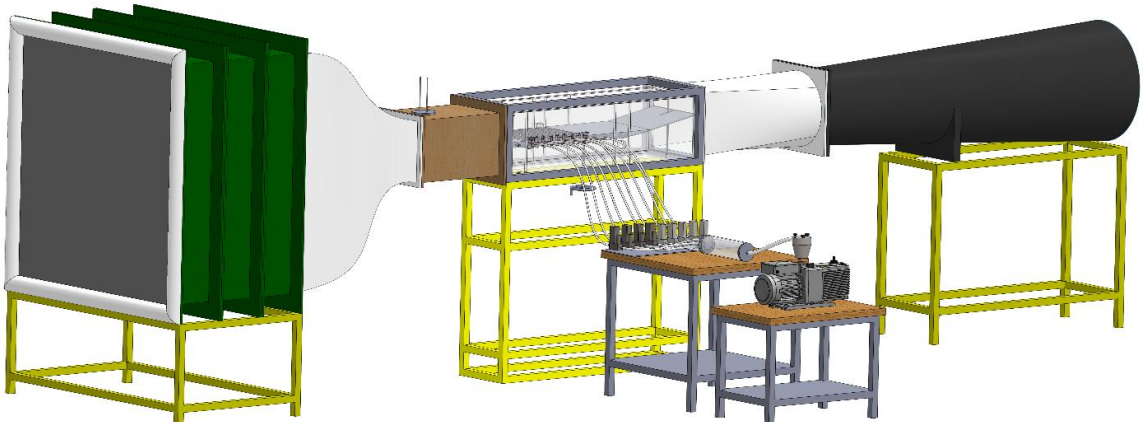

Figure 1. Overview of the ONERA TRIN2 subsonic wind tunnel facility.

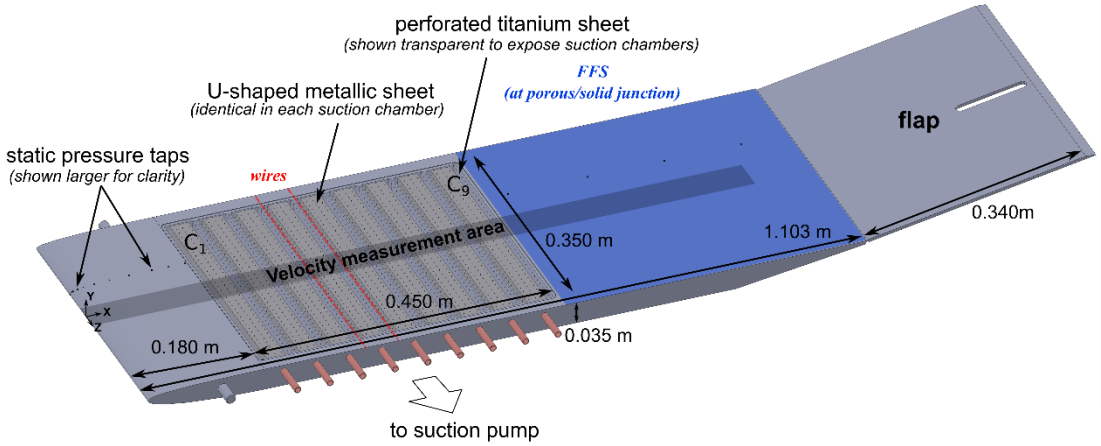

Figure 2. Overview of the flat plate and flap with all wires positions and one FFS position.

fluctuations, as calculated by Linear Stability Theory (LST).

3. REFERENCE SMOOTH CASES

In the present investigation, the nine chambers of the suction region are sealed with a 0.9 mm-thick micro-perforated titanium sheet. The perforations have a 90 µm diameter and are evenly spaced in a square pattern of dimensions 1.6 mm by 1.6 mm. The resulting porosity, defined as the ratio of the open area to the total surface of the sheet, is approximately 0.26%. Each suction chamber is connected to its corresponding mass flow meter-controller, and for all configurations the total suction mass flow rate was kept constant at 0.4g.s^{-1} while only suction distribution changed.

Four suction configurations were chosen. The first one is *no suction*, where the boundary layer is simply in contact with the porous panel mounted over the chambers but the valves of all mass flow meters are closed. The next configurations with suction are: C1/0.400, with all 0.4 g.s^{-1} concentrated on chamber C1; C3,5/0.200, where suction is equally divided in 0.2 g.s^{-1} over chambers C3 and C5; and finally, *full suction* where suction is distributed over the entire suction region (equivalent to 0.044 g.s^{-1} per chamber).

For each of these suction configurations in the smooth case (no surface defect), the transition Reynolds number are given in Tab. 1. The transition position is defined as the location where streamwise velocity fluctuations start to increase past a threshold slope value, based on streamwise hot-wire traverses at a constant altitude from the flat plate surface. As expected, the results in the table show that wall suction effectively delays the onset of transition with respect to the *no suction* configuration. In agreement with results from [4], the suction distribution also influences transition position, with configuration C1/0.400 being slightly less effective than C3,5/0.200 and *full suction*. Since the boundary layer evolves spatially in the streamwise direction, the TS instabilities are also at different stages of development. Consequently, although the C1/0.400 case has the largest local suction velocity, suction here does not seem to be applied at the streamwise position that will most effectively influence the TS instabilities. Additionally, the presence of a porous wall without suction seems to destabilize the boundary layer since the *no suction* transition for the porous panel occurs upstream of that of

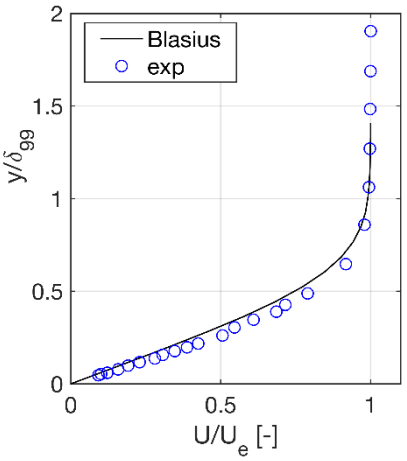

(a) Normalized boundary layer profile

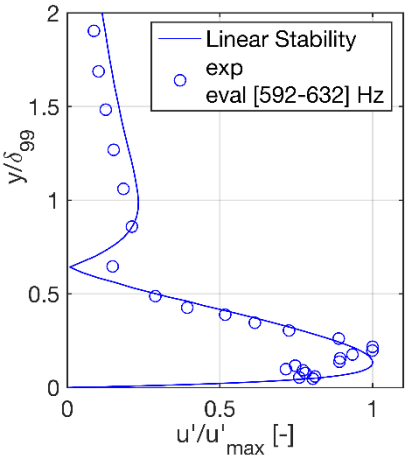

(b) TS-amplitude profile at ~ 600 Hz

Figure 3. Boundary layer and TS profiles at x = 558 mm and δ_{99}= 2.43 mm.

the solid wall panel. This effect is related to the wall impedance and is discussed in more details in [12].

Table 1. Transition positions for all suction cases with respect to the different panel porosities.

	p = 0.26%	*p = 0%*
Suction case	Re_{xT} [-]	Re_{xT} [-]
no suction	$1.66x10^6$	$1.92x10^6$
C1/0.400	$2.20x10^6$	N/A
C3,5/0.200	$2.30x10^6$	N/A
full suction	$2.30x10^6$	N/A

4. COMBINED EFFECT OF SURFACE DEFECTS AND SUCTION ON TRANSITION

In this section, the effects of wall suction combined with either wires or FFS are first characterized experimentally, and then further discussed with a numerical analysis based on linear stability theory.

4.1. Experimental characterization

The two types of positive surface defects that were tested were wires and FFS, which can both be characterized by their relative diameter or height *h* with respect to the local boundary layer thickness. Wires were tested first because of their ease of installation. Next, FFS with a rectangular edge were then mounted to investigate surface defects that were more representative of those found on aerodynamic surfaces. Although results from all the tested wires and FFS are discussed, Tab. 2 and 3 give the local boundary layer displacement thickness (calculated using ONERA's in-house boundary layer code 3C3D) at the defect location (x_{SD}) along with the corresponding relative height for selected wires and FFS, which are of particular interest. The general location of these selected defects is also shown on Fig. 2.

The transition Reynolds numbers Re_{xT} for each suction configuration and for all tested wires and FFS are summarized in Fig. 4a and 4b, respectively. For the wires, the data were compared to reference data [13] and show relatively good agreement in terms of absolute values of the transition Reynolds with the *no suction* case. For the configurations with suction, regardless of the distribution, Re_{xT} is effectively delayed with respect to *no suction* for wires with relative heights below 0.4; however, past this threshold value, all configurations then collapse onto Tani's reference curve and transition actually occurs at the wire location. Regardless of whether or not suction was applied, the wire's critical relative height is therefore approximately equal to 0.4.

For the FFS, the experimental data from the present study are compared to data from [14]. In this case, no good agreement is found between the two studies, which can be attributed to two main reasons. The first is due to the difference in freestream turbulence levels between the two wind tunnel facilities used, as can be seen by the varying Re_{xT} in the smooth case ($h/\delta_1 = 0$) from the Wang and Gaster data and the *no suction* configuration in this study. The second is related to different various positions of the FFS on the flat plate models, as highlighted by the horizontal lines on Fig. 4b. Even in the framework of the present study, the data points from the FFS that were tested at two different streamwise positions (*x* equal to 430 mm and 640 mm from the leading edge) do not collapse.

To enable comparisons between the different suction configurations to surface defects with similar values of h/δ_1, a non-dimensional parameter Δ_{xT} was then introduced in Fig. 5 and is defined as:

$$\Delta_{xT} = \frac{Re_{xT,SD} - Re_{x,SD}}{Re_{xT,noSD} - Re_{x,SD}} = \frac{x_{T,SD} - x_{SD}}{x_{T,noSD} - x_{SD}} \qquad (1)$$

Since this parameter is used for both types of surface defects, the subscript "SD" is general and stands for "Surface Defect". For any given suction configuration (and panel whenever indicated), variables $Re_{xT,SD}$ and $Re_{xT,noSD}$ correspond to the transition Reynolds number with and without a surface defect respectively, and $Re_{x,SD}$ corresponds to the location of the surface defect. The parameter Δ_{xT} can be used as an indicator of the relative change in transition position due to the presence of a surface defect, using the roughness element position as the reference. When Δ_{xT} is equal to 1, the surface defect has no effect on transition whereas when Δ_{xT} is equal to zero, transition occurs at the location of the surface defect.

Using the Δ_{xT} parameter on the wire data, the critical

Table 2. Local boundary layer displacement thickness and relative heights of selected wires.

		δ_1 [µm] at x_{SD} (from 3C3D)					
x_{SD} [mm]	wire diameter, *h* [µm]	*no suction*	C1/0.400	C3,5/0.200	*full suction*	*no suction* h/δ_1	rounded h/δ_1 (for ref.)
330	100	605	569	547	585	0.17	~0.2
430	300	692	665	611	663	0.43	~0.5

Table 3. Local boundary layer displacement thickness and relative heights of selected FFS (x_{SD} = 640 mm).

	no suction	C1/0.400	C3,5/0.200	*full suction*	
δ_1 [µm] at x_{SD} (from 3C3D) :	840	820	800	800	
FFS height h [µm]	h/δ_1				rounded h/δ_1 (for ref.)
500	0.60	0.61	0.63	0.63	~0.6
850	1.01	1.04	1.06	1.06	~1.0
1150	1.37	1.40	1.44	1.44	~1.4

relative height of 0.4 is clearly identified. Additionally, the critical relative height for the FFS can now also be found and is approximately equal to 1.3, regardless of suction configuration and step location.

In order to understand the effect of each type of defect (both subcritical and critical), the power spectral densities (PSD) of the streamwise velocity fluctuations u' slightly upstream of the corresponding transition position, along with the mean velocity boundary layer profiles 1 mm downstream of the respective defect, are shown in Fig. 6.

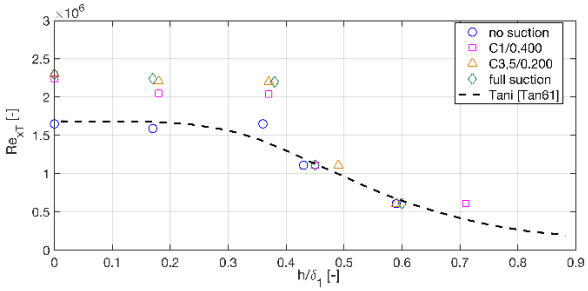

(a) Wires

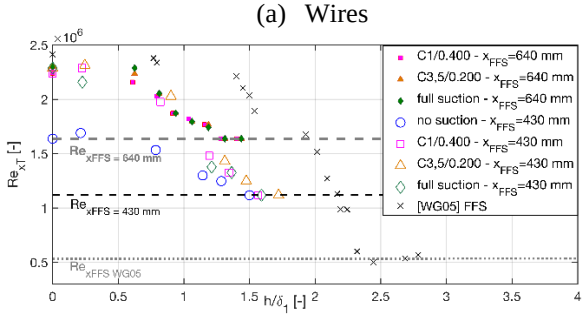

(b) FFS

Figure 4. Transition Reynolds number as a function of h/δ_1 for wires and FFS.

In Fig. 6a, the Tollmien-Schlichting instabilities can be identified as the band of amplified frequencies between 400 Hz and 800 Hz in the *no suction smooth* configuration. Similarly, close to their respective transition position, the PSD for the subcritical wire and FFS exhibit the same band of amplified frequencies, indicating that transition is still the result of the linear amplification of Tollmien-Schlichting instabilities. Although in these subcritical cases, *full suction* effectively delays the transition position with respect to *no suction*, the transition mechanism is also unchanged. Immediately downstream of the subcritical defects, Fig. 6b shows that, for each type of defect, the profiles overlap well between the two suction configurations, which seems to indicate that at this location, the effect of the surface defect on the mean flow is larger than that of suction.

In contrast, in the critical case, the transition mechanism of each type of defect is different. In the case of the critical FFS (here h/δ_1 = 1.4), the band of amplified frequencies between 400 Hz and 800 Hz that is characteristic to the Tollmien-Schlichting instabilities can be identified in the PSD of u' taken sligthly upstream of the transition position, as shown in Fig. 6c. On the other hand, the PSD of u' for the critical wire only exhibits a band of amplified frequencies between 2 kHz and 3 kHz. Upon closer inspection of the mean velocity boundary layer profiles immediately downstream of the critical wire, a well-defined inflection point can be observed. In this case, the transition mechanism has switched from being driven by viscosity to being an inflection-point instability.

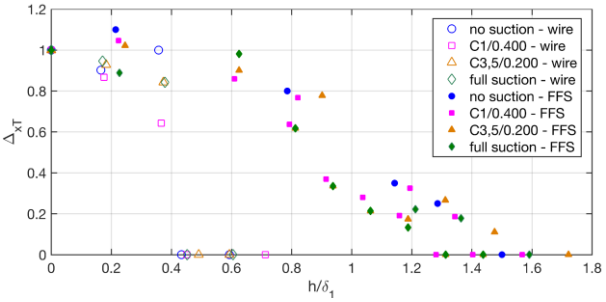

Figure 5. Comparison of the Δ_{xT} parameter for all wires and FFS.

4.2. Numerical analysis

The fact that the transition mechanism for the FFS tested in this study remained unchanged and that the range of subcritical FFS h/δ_1 is between 0 and 1.3 warrants the used of the ΔN approach. The first step to determine the ΔN values for all experimental test cases is using LST, to evaluate the maximum N factor envelope curve for the smooth case and for each suction configuration. The N_T is then determined based on the experimental transition position, and is assumed to be constant for a given

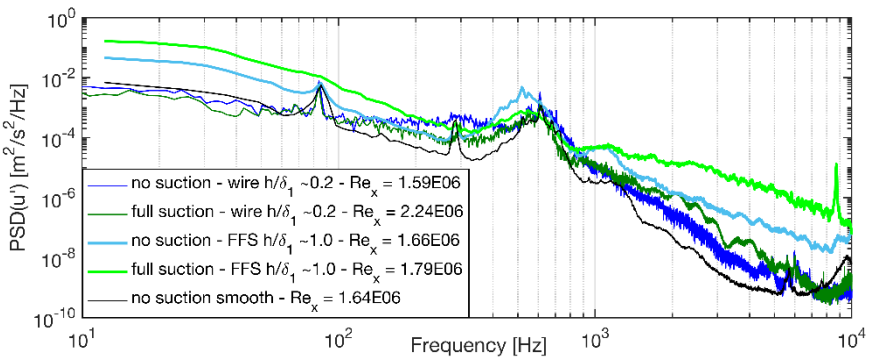

(a) PSD(u') slightly upstream of Re_{xT} (subcritical)

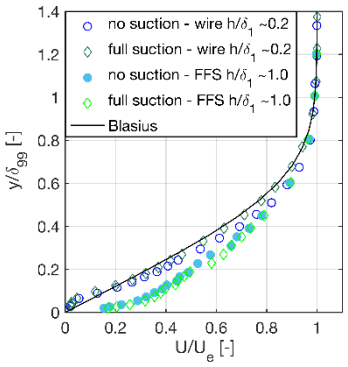

(b) Profiles 1 mm downstream of subcritical defect

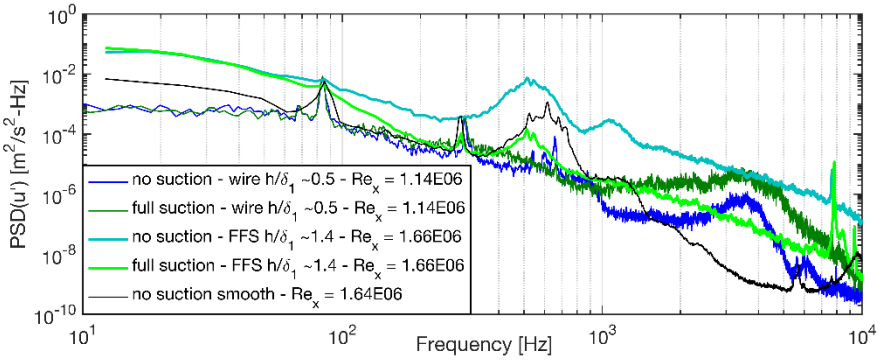

(c) PSD(u') slightly upstream of Re_{xT} (critical)

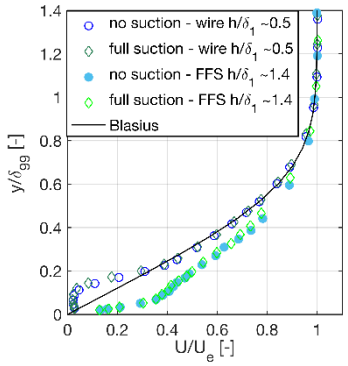

(d) Profiles 1 mm downstream of critical defect

Figure 6. Spectral analysis of the velocity fluctuations just upstream of transition location and boundary-layer profiles just downstream of the defects (wires and FFS)

suction configuration. Next the N factor at the transition position with a surface defect, $N_{xT,FFS}$ is determined using the same maximum N factor envelope curve. The ΔN is then defined as:

$$\Delta N = N_{T,smooth} - N_{xT,FFS} \qquad (2)$$

The ΔN values from the present data are plotted and compared to data sets on solid panels (i.e., without suction), both experimental by [14] and numerical by [15], in Fig. 7. Good agreement is found between the data from the literature and *no suction*, which is the most comparable case. Data from the suction configurations with x_{FFS} at 640 mm seem to match the [CKN06] model relatively well. On the other hand, for the upstream FFS position, the suction configurations have ΔN values that significantly diverge from both of the curves labeled [WG05] (for [14]) and [CKN06] ([15]).

5. CONCLUSION

An experimental investigation on the effects of wall suction combined to FFS and wires was carried out. For subcritical defect relative heights, wall suction was still found to be effective in delaying transition, albeit less effectively than in the smooth case configuration. However, the dimensions of the critical surface defects (where transition occurs at the defect location) were unchanged, regardless of whether or not suction was applied. The local change in boundary layer thickness under the influence of wall suction was therefore not significant enough to modify critical dimensions. Finally, existing ΔN model and data for FFS were in relatively good agreement with ΔN values from the present study, supporting the use of this approach for FFS both with and without suction.

6. REFERENCES

1. Joslin, R.D. (1999). Overview of laminar flow control. *NASA/TP-1998-208705*.

2. Braslow, A.L. (1999). A history of suction-type laminar flow control with emphasis on flight research. *Mon. in Aero. Hist.* **13**.

3. Reed, H.L. & Nayfeh, A.H. (1986). Numerical-perturbation technique for stability of flat-plate boundary layers with suction. *AIAA Journal*. **24**(2). DOI: 10.2514/3.9247

4. Casalis, G., Copie, M.L., Airiau. C. & Arnal, D. (1996). Nonlinear analysis with PSE approach. In: IUTAM Symposium on Nonlinear Instability and

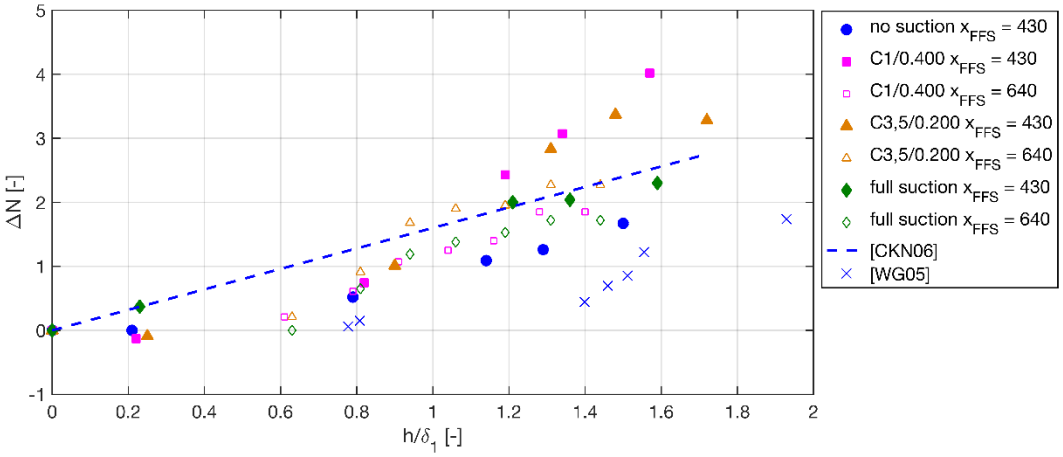

Figure 7. All suction configurations with FFS compared with Δ*N* model from [15] and with experimental data from [14].

Transition in Three-Dimensional Boundary Layers. Fluid Mechanics and Its Applications. Springer, Dordrecht, The Netherlands. DOI: 10.1007/978-94-009-1700-2_23

5. Zahn, J. & Rist, U. (2018). Study About Boundary-Layer Suction at a Juncture for Sustained Laminar Flow. In: New Results in Numerical and Experimental Fluid Mechanics XI. Notes on Numerical Fluid Mechanics and Multidisciplinary Design. Springer, Cham. DOI: 10.1007/978-3-319-64519-3_32

6. Schrauf, G. (2004). Large-scale laminar flow tests evaluated with linear stability theory. *Journal of Aircraft.* **41**(2). DOI: 10.2514/1.9280

7. Arnal, D., Reneaux, J. & Casalis, G. (1996). Numerical and experimental studies related to skin friction drag reduction problems. In: Transitional Boundary Layers in Aeronautics.

8. Nenni, J.P. & Gluyas, G.L. (1966). Aerodynamic design and analysis of an LFC surface. *Astronautics & Aeronautics.* **4**(7).

9. Béguet, S., Perraud, J., Forte, M. & Brazier, J.P. (2016). Modeling of Transverse Gaps Effects on Boundary-Layer Transition. *Journal of Aircraft.* **54**(2). DOI: 10.2514/1.c033647

10. Methel, J., Forte, M., Vermeersch, O. & Casalis, G. (2019). An experimental study on the effects of two-dimensional positive surface defects on the laminar–turbulent transition of a sucked boundary layer. *Exp. Fluids.* **60**(94). DOI: 10.1007/s00348-019-2741-2

11. Morkovin, M.V., Reshotko, E. & Herbert, T. (1994). Transition in open flow systems - A reassessment. *Bull. Am. Phys. Soc.* **39**.

12. Methel, J. (2019). An experimental investigation on the effects of surface imperfections on the laminar-turbulent transition of a boundary layer undergoing wall suction. PhD Dissertation. https://hal.archives-ouvertes.fr/tel-02408144/

13. Tani, I. (1961). Effect of two-dimensional and isolated roughness on laminar flow. In: Boundary Layer and Flow Control. DOI: 10.1016/b978-1-4832-1323-1.50004-x

14. Wang, Y.X. & Gaster, M. (2005). Effect of surface steps on boundary layer transition. *Exp. Fluids.* **39**. DOI: 10.1007/s00348-005-1011-7

15. Crouch, J.D., Kosorygin, V.S. & Ng, L.L. (2006). Modeling the effects of steps on boundary-layer transition. In: IUTAM Symposium on Laminar-Turbulent Transition. Fluid Mechanics and Its Applications. **78**. Springer, Dordrecht. DOI: 10.1007/1-4020-4159-4_4